TITLE:

Bunker consumption of containerships considering sailing speed and wind conditions

AUTHORS:

Josep R. Medina*, Jorge Molines, José A. González-Escrivá, and José Aguilar

Universitat Politècnica de València

*jrmedina@upv.es, jormollo@upv.es, jgonzale@upv.es, jaguilar@upv.es

*Corresponding author: Josep R. Medina, jrmedina@upv.es

* Building 4A, ETSI Caminos, Camino de Vera s/n, 46022 Valencia, Spain

Declarations of interest: none.

Bunker consumption of containerships considering sailing speed and wind conditions

Josep R. Medina[1], Jorge Molines[2], José A. González-Escrivá[3], and José Aguilar[4]

[1,4]Professor, [2]Assistant Prof., [3]Associate Prof., Institute of Transport and Territory, Universitat Politècnica de València; [2]jormollo@upv.es, [3]jgonzale@upv.es, [4]jaguilar@upv.es

[1]Corresponding author: Josep R. Medina, jrmedina@upv.es

ASTRACT

This study focuses on container vessel fuel consumption considering the wind conditions along the ship path in the liner route. Simple analytical and semi-empirical formulas are provided to estimate the total resistance force and the bunker consumption rate of fully loaded containerships between 5000 and 15000 TEU considering the effect of wind and the corresponding waves on the Beaufort scale. The bunker consumption rate is proportional to the total resistance force, so bad weather significantly increases fuel consumption. Examples of wind hindcasts and added resistance increases for the Atlantic Ocean, the Mediterranean Sea, and the Indian Ocean are provided for a better "a priori" estimation of the bunker consumption for a containership in a given route and time of the year.

KEYWORDS: Sea transport; container shipping; weather routing; bunker consumption; sailing speed optimization; Beaufort scale.

1. Introduction

Bunker fuel cost varies from 50% to 75% of the total operating cost of large container ships (see Ronen, 2011); the higher the fuel prices, the higher the proportion of operating costs due to bunkering. Fuel consumption in the route, type of fuel and fuel

unit price in the selected bunkering sites are the three main factors affecting bunkering cost optimization.

The prices of the different bunker fuels (IFO380, MGO, VLSFO, etc.) are highly correlated with the price of crude oil in the global market. In the short term, the fluctuation of crude oil prices and other market forces impose different fuel prices at different bunkering sites along the route of a containership, and these may be considered to optimize bunkering costs (see Aydin et al., 2017). In the long term, the progressive extension of the limits of pollutant emissions will reduce the consumption of cheap but high sulfur fuel oil (e.g. IFO380) and increase the use of cleaner but more expensive fuels (e.g. MGO or VLSFO). Furthermore, the International Maritime Organization (IMO) has been enforcing Energy Efficiency Design Index (EEDI) limits for new ships since 2011 to promote a higher efficiency in fuel consumption used for maritime transportation. Additionally, measures such as a new global sulfur cap 0.5% (from 3.5%) taking effect in 2020 and specific SOx and NOx Emission Control Areas are forcing ship owners to use cleaner but more costly fuels for maritime transportation (see Zis et al, 2019), and this increases the relevance of reduced bunker consumption which is closely related to the ship emissions. Bouman et al. (2017) reviewed around 150 studies to provide an overview of the twenty two (22) types of measures to reduce CO_2 emissions in the shipping industry; sixteen (16) types of measures (grouped in three categories: “hull design”, “power and propulsion” and “operations”) may reduce emissions by reducing fuel consumption. In this study, the attention is focused on estimate the fuel consumption of containerships taking into account the weather conditions along the ship path, which corresponds to the “voyage optimization” measure in the category of “operations” given by Bouman et al. (2017).

To estimate bunker costs, there is a variety of economic and logistic factors and models which may be considered in the optimization of the operational sailing speed and bunkering strategy of a liner shipping service (see Psaraftis and Kontovas, 2013, and Wang et al., 2019). Sailing speed optimization methods described in the literature usually assume a constant vessel speed for each leg of the liner-shipping route. It is widely accepted (e.g. Ronen, 2011, Kim, 2014, and Wang et al., 2019) that the daily fuel consumption (tonne/day) of a ship is roughly proportional to the third power of the sailing speed; if the operational speed decreases (slow steaming) in a given liner shipping service (fixed routes, ports and sailing schedules), bunker consumption and costs decrease. However, a lower operational speed usually increases other transportation costs such as the use of more ships to maintain the transportation capacity of the liner shipping service (see Notteboom and Verninmen, 2009), inventory costs, insurance, maintenance or crew costs.

The wide variety and large number of relevant variables involved in the real maritime transportation problems compels researchers and practitioners to focus on highly simplified models with limited applicability to specific applications at the operational, tactical or strategic level. Numerous sailing speed optimization methods described in the Transportation literature center on the routing problem (e.g. Fagerholt et al., 2015) and neglect sea weather conditions along the ship path. Some authors (e.g. Wang and Meng, 2012) assume the weather (rain, snow, fog, wind, waves, etc.) is an additional source of uncertainty along with port services (efficiency, handling, congestion, etc.). However, it is clear that winds, waves and other weather conditions may significantly affect fuel consumption in certain routes, and speed loss due to wind and waves is a relevant issue in weather routing (see Lin et al., 2013, Bentin et al., 2016 and Perera and

Soares, 2017). The methodology (see IMO, 2012) to calculate EEDI uses a specific coefficient to take into account the added resistance due to wind and waves, and continuous efforts are made to analyze the ship performance for weather routing applications (see Park et al., 2015, and Perera and Soares, 2017).

An intense numerical and small-scale experimental effort has been made in recent years (see ITTC, 2017) to estimate resistance due to wind and waves. Nevertheless, this research goal is far from being reached because the ship path, as well as wind and waves, may travel in different directions; waves generated by local wind (sea) are correlated to the wind but ocean waves (swell) are not correlated to the local wind. Furthermore, wind and waves not only affect resistance to the ship's motion, but also the propulsion efficiency. The complexity of the real problem of estimating the bunker consumption of a specific ship in a given weather condition compels researchers to use simplified models. The Beaufort number (BN) and the angle between wind and ship's course (see Bialystocki and Konovessis, 2016) are frequently used to characterize the weather conditions to estimate the added resistance and fuel consumption due to wind and waves. Some researchers (see Coraddu et al., 2017, and Du et al., 2019) include trim optimization along with weather conditions when predicting and optimizing the bunker consumption of real ships. Assuming calm weather in a sailing speed optimization problem may lead to a relevant miscalculation of bunker consumption.

Wind, waves and other weather variables are routinely forecasted worldwide and thus should be used to reduce uncertainty and to optimize sailing speed in liner shipping services. A specific sequence of port calls, deployed ships and designed schedules are given in advance by the liner shipping service to define precise ship routes. A liner

shipping company usually has a container fleet and a complex network involving several shipping routes with some common hub ports that allow for efficient maritime transportation between port calls in the network. At the operational level, the liner shipping service may provide additional information regarding changes to port calls and schedules (days in advance) of a given ship in the route. A reasonable objective is to minimize bunkering and other operational costs taking into consideration the weather forecast in real time, with the optimum level of service, to maximize benefits in the short term. At the strategic and tactical level, the sailing speed of containerships in different routes must be optimized to estimate the number of containerships in each leg, the travel time between port calls, the bunker consumption and other operational costs of the fleet. This study focuses on estimating the fuel consumption of a large containership considering the wind conditions along the ship path in the liner-shipping route.

1. Bunker consumption and vessel speed

A third power relationship is commonly assumed (see Ronen, 2011) between daily fuel consumption and vessel speed ($F= c\ V^3$), in line with the range of exponent 2.7 to 3.3 given by Wang and Meng (2012b) when analyzing the fuel consumption of containerships sailing below 20 knots. A similar power relationship has been used by other authors with exponent up to 4.0 and greater (see Meng et al., 2016). Yao et al. (2012) proposed a relationship $F= k_1 + k_2\ V^3$ based on data acquired from a shipping liner of container ships up to 8000 TEU. As noted by Lee et al. (2018), this empirical model for fuel consumption provide reasonably good estimations but may significantly differ from actual fuel consumption depending on weather conditions. Thus, most bunkering cost optimization methods described in the literature (see Psaraftis and Kontovas, 2013) assume a constant vessel speed between contiguous port calls in a shipping route to estimate travel time and bunker consumption between each port call. A scenario of

higher fuel prices with excess carrying capacity (lower transportation demand) makes slow steaming a reasonable option for liners to reduce costs in the short term, as occurred during the 2009 crisis and in years later. However, in the long term, it is not so clear how to optimize the vessel speed because inventory costs, crew costs and other costs increase in slow steaming.

The third power relationship between daily fuel consumption and sailing speed is related to a second power relationship between fuel consumption per nautical mile and vessel speed. This second power relationship is related to the drag force caused by the motion of a body through a fluid (water or air), which is roughly proportional to the second power of the flow velocity. Thus, the energy per unit transportation distance required to move a ship through the water and air is roughly proportional to the second power of the sailing speed. This rule-of-thumb is also valid for other vehicles transporting goods (ships, trucks, trains, etc.); in the short term, slow steaming of ships or slow velocity of trucks may be a good option to significantly reduce fuel consumption in a given transportation service. In the long term, however, a number of additional variables must be taken into consideration (freight rates, demand and carrying capacity, inventory costs, design ship speed, etc.); the sailing speed of containerships in different routes is optimized at the strategic (years) and tactical (months) levels, and finally, vessel speed is decided in real time at the operational level by the ship's captain.

This study focuses on bunker consumption considering the wind conditions along the sailing route; sea currents, swell, ice and other weather conditions are not analyzed. When wind forecasting is taken into account, sailing speed between port calls in a route should not be a constant value but it should change in time to better adapt to the forecasted weather conditions along the ship's route; however, it is not feasible to change frequently the power of the main engine of a ship. Fuel consumption (tonne per nautical mile) increases when the wind blows opposite to the ship movement, and it decreases when the wind blows in the same direction. When wind hindcast is taken into account,

the travel time between port calls and the bunker consumption of the fleet are dependent on wind conditions and must be considered by the shipping liner to estimate the number of vessels and their estimated operational costs at the tactical (months) and strategic level (years).

2.1 An analytical approximation to the total resistance force

In addition to sailing speed, there are numerous factors affecting bunker consumption during sailing (see Bouman et al., 2017, and MAN, 2018) such as engine power, propeller and hull design for a given design ship speed, hull roughness and fouling, heat recovery, shaft efficiency and other ship-related variables, as well as many safety and weather variables (wind, waves, currents, rain, ice, etc.). In this section, a simple analytical model and a semi-empirical formulae considering wind is compared to the empirical fuel consumption model given by Yao et al. (2012) to estimate the bunker consumption of containerships during sailing ($V>>0$). Besides the fuel required for navigation, a certain bunker consumption is required to maintain shipboard services which may be expressly regulated in some port areas; furthermore, the limit of emissions and type of fuel in emission control areas impose special restrictions to optimize marine routing and sailing speed (see Fagerholt et al., 2015).

In this section the three main components of resistance force to the ship's movement are selected following the classification of MAN (2018):

(1) Frictional resistance (R_F) which depends on the shape and wetted surface of the hull as well as the hull roughness (fouling, etc.); R_F is approximately proportional to the squared sailing speed, V^2.

(2) Residual resistance (R_R), depending on hull design, is associated with wave making (ship waves), eddies and viscous pressure resistance; R_R is also approximately proportional to the squared sailing speed, V^2.

(3) Air and wind resistance (R_a) corresponding to the drag force caused by the air on the ship; R_a is approximately proportional to the squared apparent air speed on the ship course, V_a^2.

Effects of wind waves will be partially considered along with wind resistance, but ocean waves (swell), ocean currents, ice and other weather variables are not considered in this study.

Bearing in mind the formulas recommended by MAN (2018) to estimate frictional and residual resistance and those recommended by ROM 2.0-11 and ROM 0.4-95 to estimate forces on mooring lines caused by wind on ships, the total resistance force including drag and viscous components of water and air can be estimated by

$$R = R_F + R_R + R_a = \frac{C_F}{2}\rho_w V^2 A_s + \frac{C_R}{2}\rho_w V^2 A_s + sgn(V_a)\frac{C_a}{2}\rho_a V_a^2 A_{Te} \quad (1)$$

in which C_F , C_R and C_a are the friction, residual and air drag coefficients, respectively, ρ_w and ρ_a are the mass density of water and air, respectively, and A_s and A_{Te} are the hull's wetted surface and the emerged cross section area, respectively. V is the sailing speed while V_a is the apparent air speed on the ship's course (V_a>0 if wind blows opposite to the ship motion). According to MAN (2018), in calm weather, R_a is relatively small and R_F is usually the dominant component for slow moving ships (e.g. tankers) while R_R is as relevant as R_F for fast moving ships. The three components are relevant for containerships sailing fast in bad weather. If the vessel is moving with a sailing speed V and course Θ_s (see Fig. 1)

$$V_a = V - V_{ws} = V - V_w\cos(\theta_s - \theta_w) \quad (2)$$

in which V_W is the wind speed, Θ_w is the wind direction, V_{ws} is the wind component on the ship's course, and V_a is the apparent air velocity to estimate the air drag force in Eq. (1). In calm weather, $R=R_0$ is the total resistance force with V_w=0 and V_a=V in (1).

If the wind is blowing opposite to the ship movement (V_{ws}<0), the air drag force increases relative to calm weather. When wind favors the ship movement (V_{ws}>0), the

air drag force decreases or, if $V_{ws}>V$, wind may even push the ship forward. Wave and wind force components perpendicular to the ship course affect ship's safety, oscillations, drag forces and may also reduce the propulsion efficiency increasing the bunker consumption.

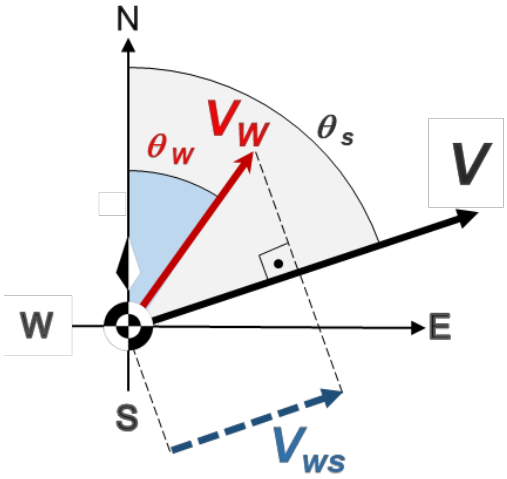

Fig. 1. Sketch showing wind direction (Θ_w), ship course (Θ_s) and the projection of the wind on the ship's course (V_{ws}).

Drag coefficients C_F, C_R and C_a and areas A_s and A_{Te} in Eq. (1) depend on the characteristics of the ship as well as the Froude and Reynolds numbers (see Kristensen and Lützen, 2012). According to MAN (2018), numerous factors affect the total water resistance of a ship in calm weather, and C_R increases when the Froude number (F_r) increases being the dominant resistant force when $F_r=V/(gL_{wl})^{0.5}>0.26$, where L_{wl} is the ship length on the waterline. Therefore, both sailing speed and ship length are relevant explanatory variables for ship resistance and bunker consumption.

The data given by ROM 2.0-11 related to fully loaded containerships between 5000 and 15000 TEU were analyzed and a good agreement was found for a 1/3-power relationship between the ship displacement volume and ship length (coefficient of

determination R^2=96%), and 2/3-power relationships for wetted surface and emerged cross section area (R^2=99%):

$$L_{wl} = 1.03L_{pp} = 6.3\nabla^{1/3} \quad (3)$$

$$A_s = 6.6\nabla^{2/3} \quad (4)$$

$$A_{Te} = 0.7\nabla^{2/3} \quad (5)$$

in which L_{wl} and L_{pp} are the ship length at the waterline and between perpendiculars, respectively, ∇ is the ship displacement volume, A_s is the wetted surface, and A_{Te} is the emerged cross section area. Additionally, a linear relationship (R^2=97%) was found between displacement and carrying capacity

$$\nabla = 28000 + 15Q \quad (6)$$

in which $\nabla(m^3)$ is the ship displacement volume and Q is the ship's carrying capacity measured in TEU. The range of application for Eqs. (3) to (6) is 5000≤ Q(TEU) ≤15000.

2.2 Estimation of the bunker consumption rate

The objective of sailing speed optimization in a liner is not reducing the bunkering costs but maximizing the benefits, being the freight rate a key variable to be compared to the unit cost of transportation. Considering that the time required to transport a container from a port of origin to the port of destination is roughly proportional to the travel distance, the unit cost of transportation is roughly proportional to that distance. Therefore, the most reasonable rates in the optimization process are those referring to TEU (freight income) and nautical miles (distanced between origin and destination). Thus, in this study the attention is focused on the bunker consumption rate, f_{cr}(kg/TEU.nm), which is also related to the EEDI index (CO_2 emission/transport work) used by IMO (2012). The bunker consumption rate is roughly proportional to the ratio between total resistant force, R given by Eq. (1), and the number of containers on board. For a given sailing speed, Eqs. (1), (4) and (5) would lead to a bunker consumption rate

roughly proportional to $\nabla^{-1/3}$; the larger the ship, the lower the f_{cr}(kg/TEU.nm). Furthermore, Eq. (3) leads to a Froude number proportional to $\nabla^{-1/6}$ and Eq. (6) to a lower ratio ∇/Q for larger containerships, which imply additional reductions in the bunker consumption rate. These physical facts might explain the global tendency to use larger containerships in liner shipping, namely, the "vessel size" measure for emission reductions noted by Bouman et al. (2017).

To estimate the bunker consumption, in addition to a good estimation of the total resistant force related to the effective towing power, it is necessary to estimate the efficiency of the sailing and propulsion system (engine, shaft, propeller, cavitation, etc.) which deliver such towing power. This study assumes the simplified fuel equation and estimation of efficiencies given by MAN (2018)

$$P_{fuel} = \frac{RV}{\eta_t} \quad ; \quad \eta_t = \eta_H \eta_o \eta_R \eta_s \eta_E \tag{6}$$

in which P_{fuel} is the power delivered burning the fuel, R is the total resistance force, V is the vessel speed and η_t is the total efficiency; η_H, η_o, η_R, η_s and η_E are the hull, propeller, rotative, shaft and engine efficiency, respectively.

The hull efficiency takes into consideration the effective towing power and the thrust power delivered by the propeller; this depends on the propeller arrangement, $0.95 < \eta_H < 1.25$, say $\eta_H \approx 1.00$ in this section. The propeller efficiency is related to sailing in open water and depends on vessel speed, thrust force and the design of the propeller, $0.55 < \eta_o < 0.7$, say $\eta_o \approx 0.65$. The rotative efficiency accounts for the effect of the hull on the actual velocity of the water flowing to the propeller, $1.00 < \eta_R < 1.07$, say $\eta_R \approx 1.00$. The shaft efficiency is the ratio between the power delivered to the propeller and the brake power of the main engine, $0.95 < \eta_s < 0.96$, say $\eta_s \approx 0.95$. Finally, the engine efficiency (see WinGD, 2016) depends on the engine design, the engine speed (typically between 60 and 80 rpm), the engine power load related to sailing speed, and other factors. This study assumes a lower calorific value of 42.7 MJ/kg (see MAN, 2018) corresponding to marine

gasoil (MGO) and 0.16 Kg/kWh for MGO (see WinGD, 2016), say $\eta_E \approx 0.53$. Thus, for large containerships, $\eta_t = \eta_H \eta_o \eta_R \eta_s \eta_E \approx 0.33$; as a rule of thumb, the thermal energy of the fuel consumed by a containership is three times the net energy corresponding to the total resistance force. The MGO bunker fuel consumption rate is

$$f_{crMGO}\left(\frac{kg}{TEU\ nm}\right) \approx \frac{P_{fuel}}{Q\ V}\ \frac{1852}{42.7\ 10^6} = \frac{R}{0.33\ Q}\ \frac{1852}{42.7\ 10^6} \tag{7}$$

in which R is the total resistance force given by Eq. (1) in N, f_{crMGO}(kg/TEU.nm) is the bunker consumption rate, P_{fuel}(J/s) is the power delivered burning the fuel, Q is the number of TEU carried by the containership and V(m/s) is the vessel speed. Using the ITTC1957 formula suggested by Molland et al. (2017), $C_F = 0.075/(\log_{10}Re-2)^2$; for large containerships $0.0013 < C_F < 0.0014$, say $C_F \approx 0.0013$. Assuming $C_a \approx 0.80$ according to ROM 0.4-95 and ROM 2.0-11, and considering Eqs. (1) to (7), the bunker consumption rate can be estimated by

$$f_{crMGO}\left(\frac{kg}{TEU\ nm}\right) \approx \frac{43}{10^6}\ \frac{G}{0.33}\ (3.3[(C_F + C_R)\ \rho_w V^2] + sgn(V_a)[0.35\ C_a\ \rho_a V_a^2]) \tag{8a}$$

$$G = \frac{\nabla^{2/3}}{Q} = \frac{15}{\nabla^{1/3}\left[1-\frac{28000}{\nabla}\right]} = \frac{\left(15+\frac{28000}{Q}\right)^{2/3}}{Q^{1/3}} \approx 22\ Q^{-0.46} \tag{8b}$$

in which $\eta_t = 0.33$ is the total efficiency and V_a is the apparent air speed on the ship course. One nautical mile (nm) is 1852 m and the range of application for Eq. (8) is $5000 \leq Q(TEU) \leq 15000$.

C_F increases with hull roughness and fouling. Adland et al. (2018) noted that periodic hull cleaning leads to a relevant reduction in the bunker consumption. Mass density of sea water depends on temperature and salinity, $1020 < \rho_w(kg/m^3) < 1030$, and mass density of air is dependent on wave breaking and spray, which may significantly increase the air mass density above $\rho_w = 1.255$ kg/m^3, usually considered at the sea level during calm weather (see ROM 0.4-95).

C_R increases with the Froude number. Assuming $C_F \approx 0.0013$, $C_a \approx 0.80$, $\rho_w \approx 1025$ kg/m^3 and $\rho_a \approx 1.255$ kg/m^3, Eqs. (3) to (8) can be used to estimate the bunker

consumption rate for containerships in the range 5000≤ Q(TEU) ≤15000. In this section, the residual coefficient is estimated by

$$C_R \approx 0.0004 + 0.11(F_r - 0.12)^2 = 0.0004 + 0.11\left(\frac{V}{\sqrt{gL_{wl}}} - 0.12\right)^2 \quad (9)$$

in which F_r is the Froude number, V is the vessel speed, g is the acceleration of gravity and L_{wl} is the ship length at the waterline. Eq. (9) is estimated using the graphic in Kristensen and Lützen (2012) corresponding to C_p=0.80 and L=6.5 $\nabla^{1/3}$; L=L_{wl} is assumed. Eq. (9) leads to C_F≈0.0007 and 0.0009 for F_r=0.19 and 0.17, respectively, corresponding to 6000 TEU and 12000 TEU containerships sailing at V=20 knots.

The bunker consumption rate of 6000 TEU containerships sailing with F_r=0.19 (V=20 knots) can be estimated by

$$f_{crMGO}\left(\frac{kg}{TEU\ nm}\right) \approx \frac{43}{10^6}\ \frac{0.40}{330}\ (3.3\ [(1.3+0.9)\ 1025\ V^2] + [0.35\ \ 0.8\ \ 1255\ V_a^2]) \quad (10a)$$

$$f_{crMGO}\left(\frac{kg}{TEU\ nm}\right) \approx \frac{43}{10^6}(9.0\ V^2 + 0.43\ V_a^2) \quad (10b)$$

in which f_{crMGO} is the bunker consumption rate (marine gasoil), V(m/s) is the vessel speed and V_a(m/s) is the apparent air speed on the ship's course. In calm weather, V_a=V=10.3 m/s (sailing speed is 20 knots), f_{crMGO}(kg/TEU.nm)≈ 0.043 which is 5% lower than the empirical estimation given by Yao et al. (2012) based on 170 daily bunker consumption data for 5001 to 6000 TEU containerships. This difference is very small considering the variety of unknown variables such as loading, hull maintenance and weather conditions of the empirical data used by Yao et al. (2012) as well as the type of fuel and a number of assumptions made in this section (e.g, η_o≈0.65, η_E≈0.53, etc.).

The approximations given in this section should be taken with caution because several other factors may significantly change the result for a given containership (hull design and maintenance, etc.). Furthermore, the use of Eq. (4) in Eqs. (8) and (10) is valid only for fully loaded containerships; if the ship is partially loaded (high proportion of

empty containers), wetted surface (A_s) is lower than the estimation given by Eq. (4) and so are the frictional and residual forces (R_F and R_R) in Eq. (1).

2.3 Added resistance force due to fouling, wind and waves

Molland et al. (2017) described the friction and pressure main components of hull resistance, wake, propellers, powering process, and many other factors, including the effect of fouling (time out of dock) and weather (Beaufort wind force scale). The use of the Admiralty coefficient implicitly assumes all the resistant components to the ship motion to be directly proportional to V^2 and $\nabla^{2/3}$ as shown in Eqs. (1), (4) and (5).

Antifouling measures cost around 5% of the fuel cost of the world fleet (see Uzun et al., 2019), and periodic maintenance is mandatory for cleaning hulls and propellers; underwater cleaning or dry-docking leads to a relevant reduction in the bunker consumption (see Adland et al., 2018). Due to biofouling, C_F may increase around 3% per month (see Molland et al., 2017) depending on seawater temperature, salinity, acidity, nutrients, light intensity and other environmental conditions (see Uzun et al., 2019).

According to seakeeping theories, there are different sources of energy dissipation in sailing ships; incident, diffracted and radiated waves as well as the corresponding wave interferences should be taken into account to properly estimate the added resistance due to waves (see Pérez-Arribas, 2007). Analytical and numerical methods are usually validated with small-scale towing-tank tests; however, the real problem is so complicated (swell waves, and wind and sea waves from different directions) that it is far from being solved. Nevertheless, the new regulations to reduce emissions are leading to more energy-efficient ships, reducing resistance in calm weather as well as added resistance due to wind and waves. Many numerical and experimental studies have been conducted to predict this weather-related added resistance (e.g. Park et al., 2015, and Luo et al., 2016). However, a recent application of numerical models validated with

combined wind-tunnel and towing-tank tests (see Wang et al., 2019) highlighted the limitations due to the scaling of wave and wind loads simultaneously, as well as a variety of model effects to reproduce realistic conditions. Thus, this study used simple analytical and semi-empirical models to estimate fuel consumption of containerships to calculate the effect of known hindcast and forecasted winds on bunker consumption in any given route and time of year.

Kwon (2008) estimated the speed loss due to added resistance in wind and waves with three factors: α (correction factor for block coefficient), μ (reduction factor for wind direction) and β (speed loss in head weather). Considering a block coefficient C_B=0.70 for containerships,

$$\frac{\Delta V}{V} = \frac{\alpha\, \mu\, \beta}{100} \tag{11}$$

$$\alpha = 3.1 - 5.3\, F_r - 12.4\, F_r^2 \quad ; \quad F_r = V/\sqrt{g\, L_{wl}} \tag{12}$$

$$\mu_{head} = 1 \quad ; \; 150^o < |\theta_s - \theta_w| \leq 180^o \tag{13a}$$

$$\mu_{bow} = 0.85 - 0.015\, (BN - 4)^2 \; ; \; 120^o < |\theta_s - \theta_w| \leq 150^o \tag{13b}$$

$$\mu_{beam} = 0.45 - 0.03\, (BN - 6)^2 \quad ; \quad 30^o < |\theta_s - \theta_w| \leq 120^o \tag{13c}$$

$$\mu_{following} = 0.2 - 0.015\, (BN - 6)^2 \quad ; \quad 0^o \leq |\theta_s - \theta_w| \leq 30^o \tag{13d}$$

$$\beta = 0.7\, BN + \frac{BN^{6.5}}{22\, \nabla^{2/3}} \tag{14}$$

in which V is the sailing speed, ΔV is the speed loss, F_r is the Froude number, L_{wl} is the ship length at the waterline, BN is the Beaufort number to characterize the weather conditions, $\nabla(m^3)$ is the ship displacement, and Θ_s and Θ_w are the ship course and wind direction, respectively. The approximation given by Eq. (14) is valid for 2≤ BN ≤7 (see Kwon, 2008). Assuming resistance (R) is roughly proportional to V^2 (see Molland et al., 2017), added resistance due to wind and waves can be estimated by

$$\frac{\Delta R}{R_0} = \left(1 + \frac{\Delta V}{V}\right)^2 \text{-1} \qquad (15)$$

in which ΔR is the added resistance due to wind and waves (swell not included), ΔR is comparable to R_a in Eq. (1) subtracting the air drag component corresponding to calm weather. For head weather, added resistance due to wind and waves (swell not included) given by Eqs. (11) to (15) is higher than that estimated by (1) using V_w(m/s)= 0.86 $BN^{1.5}$. Fig. 2 compares these two estimations for the added resistance forces, corresponding to 6000 TEU containerships.

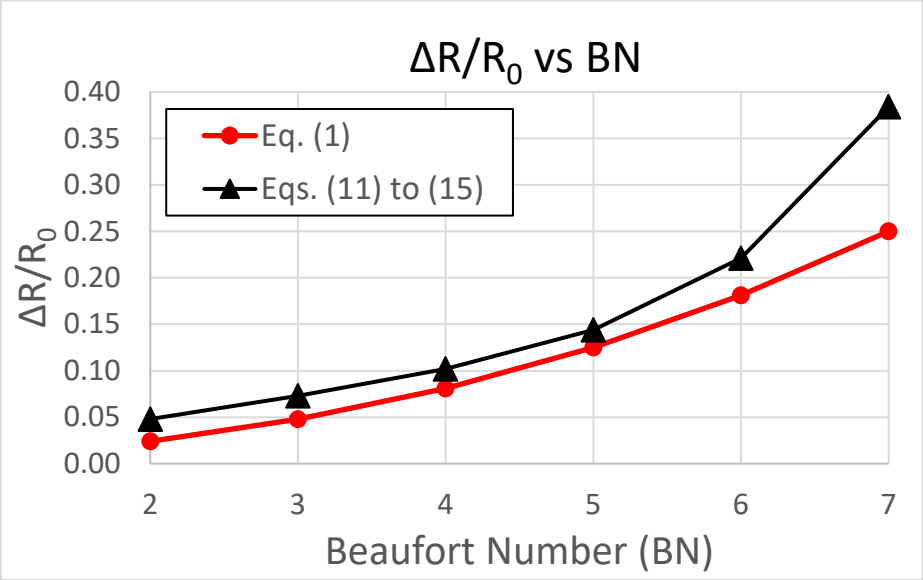

Fig. 2. Comparison of two estimations for added resistance force due to head weather for 6000 TEU containerships.

2. Bunker consumption of a typical ship route

According to Eq. (7), the bunker consumption rate f_{cr}(kg/TEU.nm) is proportional to total resistance force ($R=R_0+\Delta R$), so rough weather significantly increases fuel consumption. In calm weather, $V_w=0$ and $V=V_a$, total resistance force ($R=R_0$) and bunker consumption rate f_{crMGO}(kg/TEU.nm) can be estimated using Eqs. (1) to (9) for containerships 5000≤ Q(TEU) ≤15000. The added resistance (ΔR) due to wind and

waves (swell not included) can be estimated using Eqs. (11) to (15) which depend on Beaufort number (BN), sailing speed (V), ship course and wind direction (θ_s, θ_w) and ship displacement (∇). Eqs. (11) to (15) are applied here to evaluate the added resistance due to wind and waves of a fully loaded 6000 TEU containership travelling at an average speed of V=20 knots between Singapore and Rotterdam.

In this section 20-year hindcast wind data (1998-2018) extracted from the ERA-5 database (Copernicus Climate Change Service, 2017) are used. ERA-5 is the fifth generation of the European Centre for Medium-Range Weather Forecasts (ECMWF) atmospheric reanalysis of the global climate. The reanalysis combines model data with worldwide observations in hourly intervals with a latitude-longitude grid resolution of 0.5ºx0.5º. Hindcast wind data provide a homogeneous and consistent database. The ERA-5 wind data allow for analyses of tendencies of the historical added resistance which are valuable at the strategic level; if forecast wind data were used instead of hindcast wind data, the analysis would be analogous but the result would be valuable at the operational level.

Figure 3 illustrates the containership sailing route between Singapore and Rotterdam through the Strait of Malacca, the Indian Ocean, the Suez Canal, the Mediterranean Sea, the Strait of Gibraltar and the English Channel. Three points are analyzed along this route as representative of this shipping route: IND in the Indian Ocean, MED in the Mediterranean Sea and ATL in the Atlantic Ocean. Because the bunker consumption rate, f_{cr}(kg/TEU.nm), is proportional to total resistance force ($R=R_0+\Delta R$), the estimation of the added resistance force can be used to calculate the added bunker consumption due to bad weather.

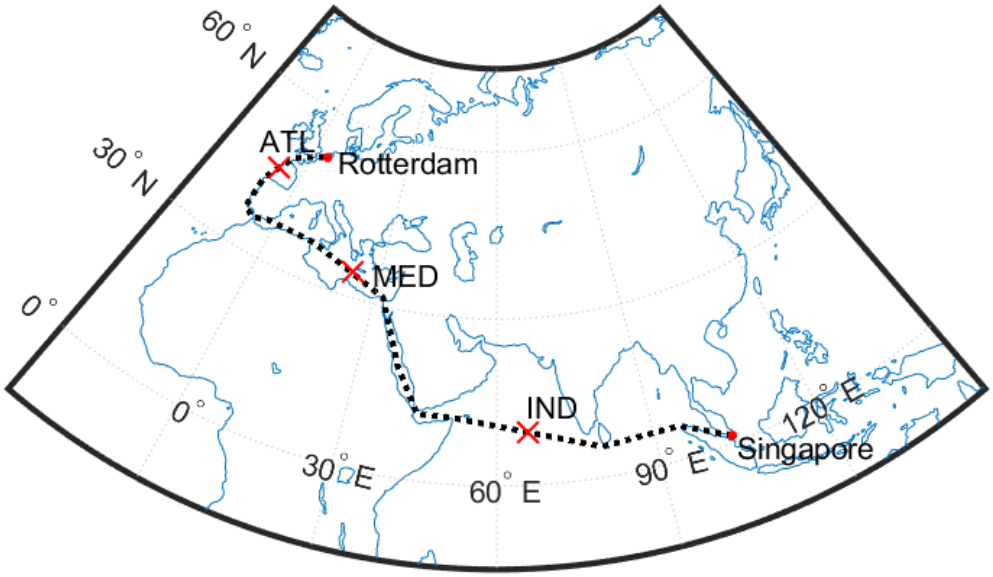

Fig. 3. Sailing route between Singapore and Rotterdam including IND, MED, and ATL.

Figures 4a, 4c and 4e illustrate the empirical cumulative distribution function, $F(\Delta R/R_0)$, of relative added resistance force ($\Delta R/R_0$) in the locations IND, MED and ATL, respectively. At these three locations, the solid lines represent the average values in the whole period 1998-2018, the dotted and dashed lines represent the average values for the months with highest median V_w^2 and lowest median V_w^2, respectively, in the period 1998-2018. The red (Northern directions) and black (Southern directions) lines identify the route from Singapore to Rotterdam and the return route, respectively.

BN<2 was considered calm weather, and $F(\Delta R/R_0)=0$ in Figures 4a, 4c and 4e indicates the probability of calm weather at each location. For each location (IND, MED and ATL), a mean ship direction is adopted to represent the shipping route in both the single and return trips: N76W-S76E in the Indian Ocean, N66W-S66E in the Mediterranean Sea and N41E-S41W in the Atlantic Ocean.

To analyze the median values of the added resistance, $F(\Delta R/R_0)=0.5$ can be used to indirectly determine the influence on the fuel consumption along the shipping route; the variations of $F(\Delta R/R_0)=0.5$ are analyzed here for the period 1998-2018 and

the months with higher and lower wind energy. Considering the period 1998-2018, the route from Rotterdam to Singapore (red lines in Fig. 4) has an median added resistance force about 80% higher due to wind and waves compared to the route from Singapore to Rotterdam (black lines in Fig. 4). Therefore, the fuel consumption of a fully loaded containership is usually higher from Rotterdam to Singapore than during the return trip.

In IND, the influence of the Monsoon wind in June is clear, with an increase in the relative median added resistance force of about 500% compared to April. In MED, an increase of approximately 100% is observed in February compared to May. In ATL, an increase of approximately 130% is observed in January compared to August. ATL shows the highest influence of the added resistance force due to wind and waves on fuel consumption.

Figures 4b, 4d and 4f describe the increases in the median relative added resistance force ($\Delta R/R_0$) depending on the ship course in the locations IND, MED, and ATL, respectively. The solid lines represent the median value of the average $\Delta R/R_0$ in the period 1998-2018, while the dotted and dashed lines represent the median value of the average values during the months with the highest V_w^2 and lowest V_w^2 in the period 1998-2018, respectively. The red lines (Northern directions) and black lines (Southern directions) indicate the mean ship direction along the shipping route in the single and return paths considered in the analysis of Figures 4a, 4c and 4e.

In IND, the Monsoon wind in June generates the highest $\Delta R/R_0$, especially when the sailing course is SW. In MED, the highest $\Delta R/R_0$ corresponds to southward sailing courses. In ATL, the highest $\Delta R/R_0$ appears when travelling southward, with a median $\Delta R/R_0$ higher than 0.04.

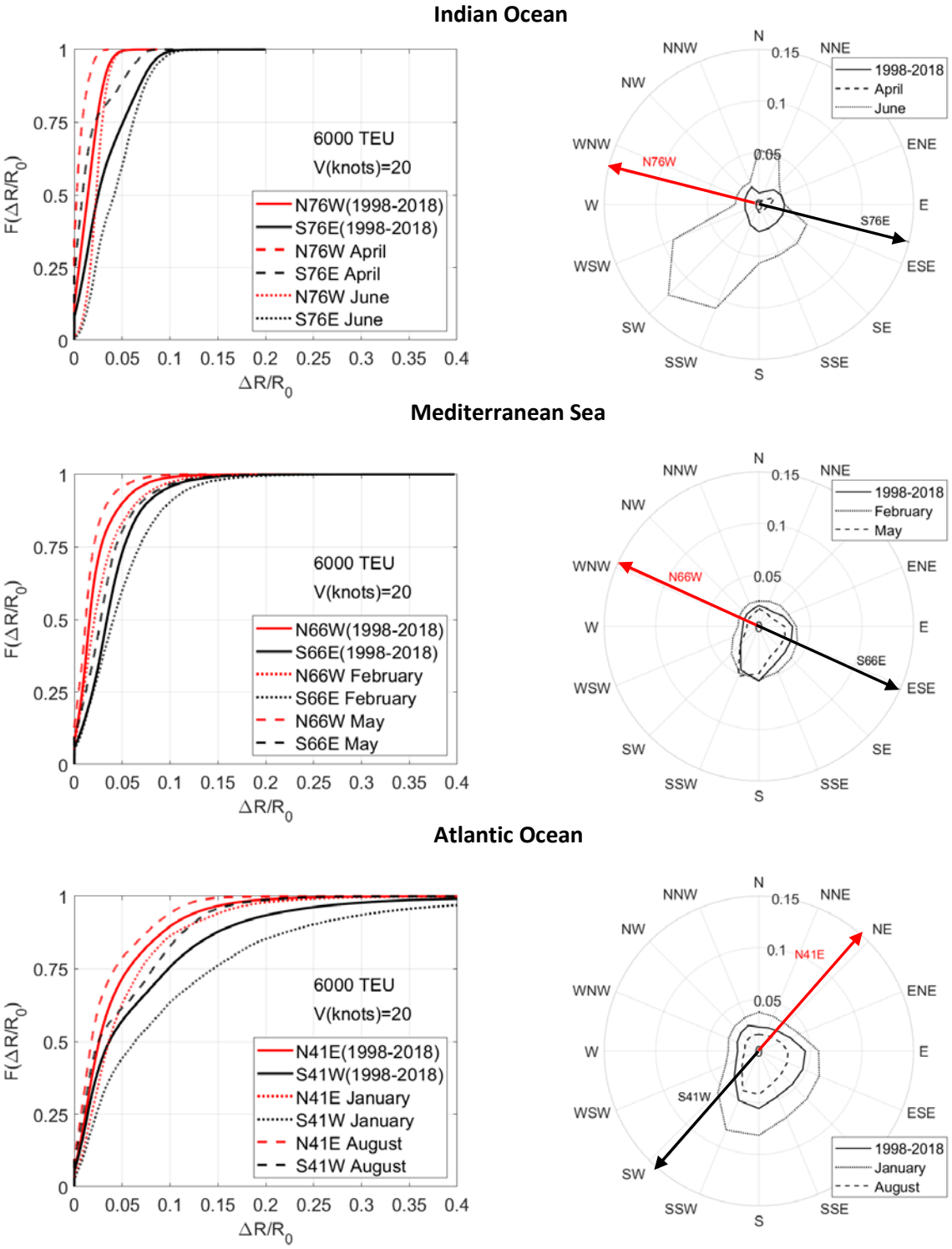

Fig. 4. Cumulative distribution function of the relative added resistance force ($\Delta R/R_0$) corresponding to points a) IND, c) MED, and e) ATL. Directional representation of the median $\Delta R/R_0$ depending on the ship course: b) IND, d) MED, and f) ATL.

Based on the results of added resistance in Figure 4, the fuel consumption due to weather in the route from Rotterdam to Singapore is higher than from Singapore to Rotterdam. There is a clear seasonal and ship route influence on the added resistance force and corresponding fuel consumption. When travelling in the Indian Ocean, the highest added resistance force appears in the SW direction in June (Monsoon period). In the Mediterranean Sea and Atlantic Ocean, travelling southward in winter increases the added resistance force by more than 100% compared to periods of calm weather.

3. Summary and conclusions

This study provides simple analytical and semi-empirical formulas to estimate the bunker consumption rate of containerships between 6000 and 15000 TEU considering the winds along the ship route. The wind and locally-generated sea waves on the Beaufort scale are used here to estimate the bunker consumption rate of containerships measured in kg of MGO per TEU and nautical mile. An analytical model and a semi-empirical model based on the formulas given by Kwon (2008) to estimate added resistance force are developed in this study to estimate the bunker consumption rate of large containerships.

The total resistance force to the ship movement, R, can be separated into frictional, residual and air components. Those components are proportional to the square of the sailing speed and apparent air velocity, respectively; these drag forces require a net towing force generated by the propulsion system when burning the fuel with a certain efficiency. For large containerships, as a rule of thumb, the thermal energy of the fuel consumed by a containership is three times the net energy corresponding to the total resistance force.

Empirical formulas are provided to estimate the ship length (at the waterline and between perpendiculars), the wetted surface and the emerged cross section area

depending on the ship's carrying capacity measured in TEU which are valid for fully loaded containerships between 5000 and 15000 TEU. The estimation of the bunker consumption rate given in this study for 6000 TEU containerships provided results similar to those by the empirical estimation found in Yao et al. (2012) based on 170 daily bunker consumption data for 5001 to 6000 TEU containerships.

The added resistance generated by wind and locally-generated sea waves can be obtained using the model by Kwon (2008) based on the Beaufort Number and compared with the analytical model by subtracting the air drag component corresponding to calm weather. Given a 6000 TEU containership travelling at 20 knots, both models provide very similar added resistance values for Beaufort Numbers between 2 (light breeze) and 7 (high wind, moderate gale, near gale). The analytical model provides slightly lower values since it only considers the wind action, while the Kwon (2008) model considered both the wind and the wind wave (sea waves) action. No models consider the influence of the ocean waves (swell waves) and other climatic variables (currents, fog, ice, or the like).

The added resistance model by Kwon (2008) is applied to a fully loaded 6000 TEU containership travelling at 20 knots between Singapore and Rotterdam considering 20 years of hindcast wind data. The route from Rotterdam to Singapore has about an 80% higher added resistance force due to wind and waves on average compared to the reverse route from Singapore to Rotterdam; therefore, the added fuel consumption due to weather is higher from Rotterdam to Singapore. There is a clear seasonal and ship route influence on the added resistance force and corresponding fuel consumption. The Indian Ocean provides the highest added resistance force when travelling southwestward in June (Monsoon period) while in the Mediterranean Sea and Atlantic Ocean, travelling southward in winter increases more than 100% the added resistance force compared to travel in months with calm weather.

The added resistance due to wind and waves has a clear influence on bunker consumption. At the operational level, the information about the forecasted winds can be used to optimize the vessel speed and route according to real-time changes in port call schedules. At the strategic and tactical level, the wind and wave hindcast climate information can be used by the ship liner to better estimate the bunker consumption of the transportation network throughout the year.

4. ACKNOWLEDGEMENTS

The authors thank the two anonymous reviewers for their constructive comments and suggestions. The authors thank Debra Westall for revising the manuscript.

Funding: This work was supported by the *Ministerio de Economía y Competitividad, Spain,* and *Fondo Europeo de Desarrollo Regional* FEDER, EU [grant RTI2018-101073-B-I00].

5. REFERENCES

Adland, R.A., Cariou, P., Jia,H. and Wolff, F.-C., 2018. The energy efficiency effects of periodic ship hull cleaning. *Journal of Cleaner Production*, 178 (2018) 1-13.

Aydin N., Lee, H. and Mansouri, S.A., 2017. Speed optimization and bunkering in liner shipping in the presence of uncertain service times and time windows at ports. *European Journal of Operational Research* 259 (1), 143–154.

Bentin, M., Zastrau, D., Schlaak, M., Freyre, D. Elsner, R. and Kotzur, S., 2016. A new routing optimization tool-influence of wind and waves on fuel consumption of ships with and without wind assisted ship propulsion systems. *Transportation Research Procedia*, 14 (2016) 153-162.

Bialystocki, N. and Konovessis, D., 2016. On the estimation of ship's fuel consumption and speed curve: A statistical approach. *Journal of Ocean Engineering and Science* 1(2016), 157-166.

Bouman, E.A., Lindstad, E., Rialland, A.I. and Strømman, A.H., 2017. State-of-the-art technologies, measures, and potential for reducing GHG emissions from shipping - A review. *Transportation Research Part D* 52 (2017), 408-421.

Copernicus Climate Change Service (C3S), 2017. ERA5: Fifth generation of ECMWF atmospheric reanalyses of the global climate. Copernicus Climate Change Service Climate Data Store (CDS), https://cds.climate.copernicus.eu/cdsapp#!/home. (accessed March 5th, 2020).

Coraddu, A., Oneto, L., Baldi, F. and Anguita, D., 2017. Vessel fuel consumption forecast and trim optimization: A data analytics perspective. *Ocean Engineering*, 130 (2017) 351-370.

Du, Y., Meng, Q., Wang, S. and Kuang, H., 2019. Two-phase optimal solutions for ship speed and trim optimization over a voyage using voyage report data. *Transportation Research Part B*, 122 (2019) 88-114.

Fagerholt, K., Gausel, N.T., Rakke, J.G. and Psaraftis, H.N., 2015. Maritime routing and speed optimization with emissions control areas. *Transportation Research Part C*, 52 (2015) 57-73.

International Maritime Organization, 2012. Interim guidelines for the calculation of the coefficient fw for decrease in ship speed in a representative sea condition for trial use. MEPC.1/Circ.796.

International Towing Tank Conference, 2017. Final report and recommendations of the Seakeeping Committee. *Proceedings of the 28th ITTC*, Vol. I, 213-273.

Kim, H.-J., 2014. A Lagrangian heuristic for determining the speed and bunkering port of a ship. *Journal of the Operational Research Society* 65 (2014), 747–754.

Kristensen, H.O. and Lützen, M., 2012. Prediction of resistance and propulsion power of ships. Project no. 2010-56, Report no. 04, October 2012. https://www.mek.dtu.dk/english/sections/fvm/software/ship_emissions (accessed February 19th, 2020).

Kwon, Y.J., 2008. Speed loss due to added resistance in wind and waves. *The Naval Architect*, RINA, London (UK), 14-16.

Lee, H., Aydin, N., Choi, Y., Lekhavat, S. and Irani, Z., 2018. A decision support system for vessel speed decision in maritime logistics using weather archive big data. *Computers and Operations Research*, 98 (2018) 330-342.

Lin, Y.-H., Fang, M.-C. and Yeung, R.W., 2013. The optimization of ship weather-routing algorithm based on the composite influence of multi-dynamic elements. *Applied Ocean Research*, 43 (2013) 184-194.

MAN, 2018. Basic principles of ship propulsion. MAN Energy Solutions, publication no. 5510-0004-04, Copenhagen (Denmark), 68 p. https://marine.man-es.com (accessed February 19th, 2020).

Meng, Q. , Du, Y. , Wang, Y. , 2016. Shipping log data based container ship fuel efficiency modeling. *Transportation Research Part B*, 83 (2016), 207–229.

Molland , A. F., Turnock, S.R. and Hudson, D.A., 2017. *Ship Resistance and Propulsion*. Cambridge University Press, UK, pp. 12-83.

Notteboom, T.E. and Verninmen, B., 2009. The effect of high fuel costs on liner service configuration in container shipping. *Journal of Transport Geography* 17 (2009), 325–337.

Park, D.-M., Lee, J. and Kim, Y., 2015. Uncertainty analysis for added resistance experiment of KVLCC2 ship. *Ocean Engineering*, 95 (2015) 143-156.

Perera, L.P. and Soares, C.G., 2017. Weather routing and safe handling in future of shipping. *Ocean Engineering*, 130 (2017) 684-695.

Perera, L.P. and Mo, B., 2018. Ship speed power performance under relative wind profiles in relation to sensor fault detection. *Journal of Ocean Engineering and Science* 3 (2018), 355–366.

Pérez-Arribas, F., 2007. Some methods to obtain the added resistance of a ship advancing in waves. *Ocean Engineering*, 34 (2007) 946-955.

Psaraftis, H.N. and Kontovas, C.A., 2013. Speed models for energy-efficient maritime transportation: A taxonomy and survey. *Transportation Research Part C* 26 (2013), 331–351.

ROM 0.4-95, 1995. *Recomendaciones para obras Marítimas. Acciones climáticas II: Viento*. Puertos del Estado (Madrid, Spain), Sep. 1995, pp. 85-145 (in Spanish).

ROM 2.0-11, 2011. *Recomendaciones para el proyecto y ejecución en Obras de Atraque y Amarre* (Vol. II). Puertos del Estado (Madrid, Spain), June 2012, pp. 240-397 (in Spanish).

Ronen, D., 2011. The effect of oil price on containership speed and fleet size. *Journal of the Operational Research Society* 62 (2011), 211-216.

Uzum, D., Demirel, Y.K., Coraddu, A. and Turan, O., 2019. Time-dependent biofouling growth model for predicting the effects of biofouling on ship resistance and powering. *Ocean Engineering*, 191 (2019) 106432.

Wang, S. and Meng, Q., 2012a. Liner ship route schedule design with sea contingency time and port time uncertainty. *Transportation Research Part B* 46 (2012) 615–633.

Wang, S., Meng, Q., 2012b. Sailing speed optimization for containerships in a liner shipping network. *Transportation Research Part E*, 48 (2012), 701–714.

Wang, S., Gao, S., Tan, T. and Yang, W., 2019. Bunker fuel cost and freight revenue optimization for a single liner shipping service. *Computers and Operations Research* 111 (2019), 67–83.

Wang, W., Wu, T., Zhao, D., Guo, C., Luo, W. and Pang, Y., 2019. Experimental–numerical analysis of added resistance to container ships under presence of wind–wave loads. *PLoS ONE* 14(8) e0221453. https://doi.org/10.1371/journal.pone.0221453.

WinGD, 2016. Engine selection for very large container vessels. WinGD Paper modified May 2nd, 2018, 18 p. https://www.wingd.com/en/news-media/media-papers/ (accessed February 19th, 2020).

Yao, Z., Ng, S.H. and Lee, L.H., 2012. A study on bunker fuel management for the ship- ping liner services. *Computers & Operations Research,* 39 (5) 1160–1172.

Zis, T.P.V., Psaraftis, H.N., Panagakos, G. and Kronbak, J., 2019. Policy measures to avert possible modal shifts caused by sulphur regulation in the European Ro-Ro sector. *Transportation Research Part D* 70 (2019), 1-17.